

FINAL
IN-35-CR
4061
22 p

FINAL TECHNICAL REPORT

**FOR
NCC 3 231**

STEREO IMAGING BASED PARTICLE VELOCIMETER

**SUBMITTED BY
CELAL BATUR
DEPARTMENT OF MECHANICAL ENGINEERING
THE UNIVERSITY OF AKRON
AKRON OHIO 44325-3903**

**SUBMITTED TO
NASA LEWIS RESEARCH CENTER
GRANTS OFFICER,
MAIL STOP 500-315
21000 BROOKPARK ROAD
CLEVELAND OHIO 44135**

**MARRY JO MYER
PROCESSING SCIENCE AND TECHNOLOGY BRANCH
MAIL STOP 105-1
21000 BROOKPARK ROAD
CLEVELAND OHIO 44135**

**NASA SCIENTIFIC AND TECHNOLOGY FACILITY
P.O. BOX 8757
BWI AIRPORT
MD 21240**

**OFFICE OF NAVAL RESEARCH
RESIDENT REPRESENTATIVE
1960 KENNY ROAD
COLUMBUS OH 42310-1063**

N94-29742

Unclas

G3/35 0004061

(NASA-CR-195800) STEREO IMAGING
BASED PARTICLE VELOCIMETER Final
Technical Report (Akron Univ.)
22 p

STEREO IMAGE MATCHING BY HOPFIELD TYPE NEURAL NETWORK

Batur, C.¹
Department of Mechanical Engineering
University of Akron
Akron - Ohio 44325-3903

4/16/94

NOMENCLATURE

$\nabla^2 G(x,y)$	Laplacian of Gaussian filter
σ	Size of the LOG filter
E	Preformance index minimized by the Hopfield network
V_{ij}	Output of neuron (ij).
C_{ij}	Compatibility measure
W	Weghts used in the compatibility measure
f_1	Distance compatibility factor
f_2	Environment compatibility factor
f_3	Location compatibility factor
λ	Steepness parameter for the compatibility curve $F(\cdot)$
θ	Offset parameter for the compatibility curve $F(\cdot)$
$sim, nsim$	Similarity and non-similarity measures
a_{mn}^i, b_{mn}^j	Elements of environment matrices
O_{1i}	Coordinates of object points on calibration plane 1
I_{1i}	Coordinates of image points of object points on plane 1
$h(\cdot)$	Calibration polynomial

KEYWORDS

Stereo imaging, matching problem, Hopfield neural network.

ABSTRACT

Three dimensional coordinates of an object are determined from it's two dimensional images for a class of points on the object. Two dimensional images are first filtered by a Laplacian of Gaussian (LOG) filter in order to detect a set of feature points on the object. The feature points on the left and the right images are then matched using a Hopfield type optimization network. The performance index of the Hopfield network contains both local and global properties of the images. Parallel computing in stereo matching can be achieved by the proposed methodology.

1. INTRODUCTION

Finding three dimensional coordinates of an object with respect to a given coordinate system is an important task in motion control and manufacturing. The basic

¹ for correspondance

motivation of this paper is to introduce a Hopfield type neural network for the solution of matching problem in stereo imaging. A typical stereo image processing starts with the acquisition of left and right images of an object. These images are processed to detect the object boundaries or a class of interesting points. Due to disparity, a point on the object projects itself to different locations in image planes. Since we have only the projected image points, the construction of the object point requires that a point on the left image should be matched to its corresponding image point on the right image. The contribution of this paper is to use a Hopfield type neural network as an optimization tool to accomplish the matching process.

The use of Hopfield neural network to parallelize the matching algorithm is earlier proposed in [1], [2]. In [2] they determined a class of interesting points on which the neural network based matching algorithm works. These interesting points are the ones that have the largest variations of gray tones around them. The matching of interesting points is accomplished by defining a quadratic optimization function which attains its global minimum at matching points. Following **Figure 1**, it is assumed that:

- a) the point (i) on the left image matches point (k) on the right image, and simultaneously,
- b) the point (j) on the left image matches point (l) on the right image.

Under these conditions, a quadratic optimization function is defined as

$$E = f\{(d_{ij} - d_{kl}), (D_{ik} - D_{jl})\} + (\text{uniqueness conditions}) \quad (1.1)$$

where d_{ij} denotes the distance between points i and j observed in images and D_{ik} is the difference in disparities between points i and k. The uniqueness conditions encourage the matching of one pair of point (i,j) on the left image to only one pair of point (k,l) on the right image. The Hopfield neural network is structured such that the quadratic optimization function E serves as a Lyapunov function for the equations that represent the neural network. Therefore, the Hopfield network is always stable and the steady state output of the network corresponds to optimum match.

The optimization function proposed by [2] has the following limitations:

- (1) Only local properties such as disparity and distance are considered. For example, referring to **Figure 1**, the disparity ($L'-L''$) and the distance ($d_{ij}-d_{kl}$) are considered.
- (2) The matching must be performed for a pair of points, i.e., if point (i) matches point (k) then simultaneously, point (j) should match point (l).

The basic idea in this paper is to improve the first condition by introducing a global property into the performance index. This global property states that if the point (i) on the left image is a match for the point (k) on the right image then lines passing through these points and the focal points should intersect. If camera lenses do not have precise focal points, as in the case of most real life cameras, then the distance between these lines should be the smallest in comparison to other pair of lines. This concept is also illustrated in **Figure 1**.

The second limitation stated above stems from the need that the performance index (1.1) must be quadratic if the Hopfield neural network is to be used. However, we will show that the performance index can still be kept quadratic if we try to match only one point on the left image to another single point on the right image. This procedure is much

more intuitive and there is essentially no need to consider the matching process for a pair of points.

The paper is organized as follows. The feature based stereo vision is presented in Section 2. The problem of matching left image points to right image points is solved in Section 3. Determination of three dimensional coordinates of the object points is given in Section 4. The example in Section 5 illustrates the methodology. Finally, the conclusions are stated in Section 6.

2. FEATURE BASED STEREO VISION

Feature based stereo imaging algorithms extract the feature primitives in each image and match these primitives according to a pre-determined criterion. Choices of primitives and matching criteria give rise to several feature based stereo algorithms. Curve segments [8], straight lines [9], corners [7] and points surrounded by high gray level variances [10] are some of the primitives used in the literature. In this study a class of edge points are used as the feature primitives. These edge points are determined by filtering both the left and the right images by the Laplacian of Gaussian (LOG) filter.

The LOG filter is a two dimensional operator given by,

$$\nabla^2 G(x,y) = \left(\frac{r^2 - 2\sigma^2}{\sigma^2} \right) \exp \left(\frac{-r^2}{2\sigma^2} \right) \quad (2.1)$$

where $r = \sqrt{x^2 + y^2}$ and σ is the size of the filter. The arguments x and y are the horizontal and vertical locations where the LOG filter operates. The filter has a value of zero at the edges and has a negative central region, as shown in Figure 2. The diameter of the negative central region, W_{2D} is directly proportional to σ , i.e., ($\sigma = W_{2D}/2\sqrt{2}$).

Since a digitized image consists of a finite number of pixels, (480 in y direction and 512 in x direction), the numerical implementation of the LOG filter can be performed only on a finite number of (x,y) locations. To ensure that the filter response is almost zero at the edges, a circular mask with dimension of $(1.8W_{2D} \times 1.8W_{2D})$ is introduced. The filter operates only within this mask and at the edges of the mask the magnitude of the filter is $\sim 5 \times 10^{-5}$. The LOG filter is also normalized such that the volume in the negative region equals the volume in the positive region. The purpose of normalization is to make sure that the output of the filter is zero when it is operating in a region where the gray level of pixels are all identical.

The (LOG) filter is used to detect the location of sudden intensity changes (edge points) on an image. The Laplacian part of the filter is a second order spatial derivative of the image whereas the Gaussian part low pass filters the image before the second order derivatives are evaluated [11]. Changing σ varies the amount of low pass filtering and therefore, affects the sensitivity of edge point detection process.

As illustrated on a one dimensional edge in Figure 3, the second order derivative of the gray level curve crosses zero around the edge. Therefore, the location of edge

points can be detected by examining the sign changes in the LOG convolved images. The sign changes can be categorized according to the direction in which they are detected, i.e., from negative to positive or visa versa. This direction information can be used as an additional property of the edge point.

The zero crossings that are not originated from a real edge are considered as noise induced zero crossings. It is desired to eliminate these noise induced zero crossings without any loss of valuable information. One practical solution to this problem is to use LOG filters with a wide bandwidth i.e., large σ . However, very large sized LOG filters may also cause elimination of real zero crossings. Another disadvantage of using a large filter is the shift of the location of zero crossing with respect to the location of actual edge. This results in a distortion of the determined shape of an object as illustrated in [3].

We use a class of edge points as the feature points for our stereo matching algorithm. Consideration of only a certain class of edge points stems from the fact that the use of all edge points leads to an excessively large neural network. The class of edge points is defined in Section 3.

3. MATCHING

Feature points are matched with a Hopfield type neural network. This network minimizes the following quadratic performance index.

$$E = -A \sum_{i=1}^{N_l} \sum_{j=1}^{N_r} C_{ij} V_{ij}^2 + \sum_{i=1}^{N_l} (1 - \sum_{j=1}^{N_r} V_{ij})^2 + \sum_{j=1}^{N_r} (1 - \sum_{i=1}^{N_l} V_{ij})^2 \quad (3.1)$$

The performance index is designed to attain its minimum value if a feature point (i) on the left image matches a feature point (j) on the right image. The first term contains (C_{ij}) $(-1 \leq C_{ij} \leq +1)$ as a compatibility measure between a feature point (i) on the left image and a feature point (j) on the right image. If the points are compatible (C_{ij}) approaches 1 otherwise, to -1. The compatibility measure is defined explicitly later in this section. The term (V_{ij}) denotes the output of neuron (ij). The neurons are assumed to have saturation type non-linear functions such that the output of a neuron is either zero or one. (N_l) and (N_r) are the number of feature points on the left and right images respectively and (A) is a user specified positive constant. The negative contribution of the first term will be at the maximum level if the output of the neuron (V_{ij}) is the largest (+1) and the compatibility (C_{ij}) is also the largest (+1).

The second and third terms in the index are introduced to enforce the uniqueness constraint in matching i.e., a point (i) on the left image can only match one point (j) on the right image. Therefore, if the neuron outputs are collected in a matrix $\{ V_{ij} \ i=1,2,\dots,N_l \ j=1,2,\dots,N_r \}$ then, for uniqueness, there should be only one element with (+1) value on a given row and column. Note that the second and the third term penalize rows and columns if they contain more than one element with (+1) value but they cannot impose the uniqueness condition exactly.

The compatibility of a feature point (i) on the left image to feature point (j) on the right image is defined by

$$C_{ij} = W1f1_{ij} + W2f2_{ij} + W3f3_{ij} \quad (3.2)$$

Where

- $(f1_{ij})$ is the compatibility factor in terms of the minimum distance between the lines of sight of the feature points (i) and (j).
- $(f2_{ij})$ is the compatibility factor in terms of the environment around the feature points (i) and (j).
- $(f3_{ij})$ is the compatibility in terms of the vertical location of the feature points on their corresponding image planes.
- $W1, W2,$ and $W3$ are the user specified weights that measure the contribution of each term. For convenience, $W1+W2+W3=1$.

We will now describe how each contributing factor in (3.2) is determined.

A - Minimum Distance Compatibility Factor ($f1_{ij}$)

The distance between the lines of sight is a global property of matching in a sense that for an ideal match this distance should be zero as illustrated in **Figure 1**.

The $(f1_{ij})$ is determined by:

$$f1_{ij} = F(dist_{ij}) \quad (3.3)$$

where $(dist_{ij})$ is the minimum distance between the lines of sight of feature point (i) on the left image and the feature point (j) on the right image. The function $F(x)$ is a sigmoid function, assigned as below,

$$F(x) = \left(\frac{2}{1 + e^{-(\theta - x)\lambda}} - 1 \right) \quad (3.4)$$

where λ a positive constant which effects the steepness of the curve as shown in **Figure 4**. The positive parameter θ shifts the curve to the right by θ . In order to normalize $(f1_{ij})$ between -1 and +1 at the maximum and minimum values of its argument, we determine λ and θ by solving the following equations simultaneously

$$\begin{aligned} F(\min(dist_{ij})) &= \frac{2}{1 + e^{-(\theta_i - \min(dist_{ij})\lambda_i)}} - 1 = 0.99 \\ F(\max(dist_{ij})) &= \frac{2}{1 + e^{-(\theta_i - \max(dist_{ij})\lambda_i)}} - 1 = -0.99 \end{aligned} \quad (3.5)$$

The variable $(\min(dist_{ij}))$ denotes the minimum value at the (row (i)) of $\{dist_{ij}\}_{i=1..N_l, j=1..N_r}$ matrix and θ_i and λ_i are the values of θ and λ for the row (i). The matrix $\{dist_{ij}\}$ contains the calculated distances between the sight vector of point (i) and the sight vector of point (j). The values of $(\min(dist_{ij}))$ and $(\max(dist_{ij}))$ depend on the experimental conditions as illustrated in Section 5.

B - Environment Compatibility Factor ($f2_{ij}$)

The second factor in the compatibility measure, i.e. ($f2_{ij}$), quantifies the dissimilarity of environments around the potential matching points (i) and (j). It is calculated by

$$f2_{ij} = F(ns_{ij}) \quad (3.6)$$

where the function $F(x)$ has the same form as in (3.4), (ns_{ij}) is a measure of dissimilarity between the environments surrounding point (i) of the left image and the point (j) of the right image. The dissimilarity (ns_{ij}) is determined by the following procedure.

Step 1. The digitized left and right images are convolved with a suitable LOG filter.

Step 2. In each filtered image, every row is examined from left to right for zero crossings. If a zero crossing is detected with a sign change from positive to negative then the pixel at this zero crossing is assigned to category 1. If the zero crossing is from negative to positive then this pixel is assigned to category 2.

Similarly, every column in each filtered image is examined from top to bottom for zero crossings. If they are not detected previously, the positive to negative zero crossings are assigned to category 3 and negative to positive zero crossings to category 4. The basic motivation here is to use the category numbers to describe the character of zero crossings. The category numbers effectively characterize the slopes around the zero crossings.

In order to reduce the number of points to match, only a class of zero crossing points are considered for matching. This class consists of zero crossing points on five horizontal lines in the image. Scanning from the top of the image, the first line is chosen as the line that contains at least one zero crossing point of category one. The last line is the line that also contains at least one zero crossing of category one. The other three lines divide the distance between the first and the last line into four equal segments. The zero crossing points with category 1 are considered as feature points to be matched. Note that the proposed reduction in the number of zero crossing points is not necessary but only convenient in order to reduce the work load of the neural network. A similar reduction is also performed in [2].

Step 3. For each feature point on the left image, an environment matrix $E_l \in R^{3 \times 15}$ is constructed. This matrix is centrally located on the feature point and contains the category numbers for zero crossings around and including this feature point. Similarly, for each feature point on the right image, an environment matrix $E_r \in R^{3 \times 15}$ is defined. Let (a_{mn}^i) denote any element in environment matrix of feature point (i) and (b_{mn}^j) denote any element in environment matrix of feature point (j).

Step 4. In order to quantify the environment around feature points, a similarity measure (sim_{ij}) is defined between the feature point (i) on the left image and the feature point (j) on the right image. For every non-zero element in the environment matrix of point (i) the same address in the environment matrix of point (j) is checked. The following procedure describes how the similarity is quantified.

$$\begin{aligned}
sim_{ij}(old) &= 0 \\
sim_{ij}(new) &= sim_{ij}(old) + 4 \quad \text{if } a_{mn}^i = b_{m,n}^j \quad m = 1..3 \quad n = 1..15 \\
sim_{ij}(new) &= sim_{ij}(old) + 2 \quad \text{if } a_{mn}^i = b_{m+1,n+1}^j \quad m = 1..3 \quad n = 1..15
\end{aligned} \tag{3.7}$$

Step 5. Finally, the dissimilarity measure between the environments is calculated as

$$ns_{ij} = 4 * n - sim_{ij} \tag{3.8}$$

where n is the number of non-zero elements in the environment matrix of point (i).
With (3.6) and (3.8), $(f2_{ij})$ can now be determined as

$$f2_{ij} = F(ns_{ij}) = \frac{2}{1 + e^{-(\theta_i - ns_{ij})\lambda}} \tag{3.9}$$

where the parameters of the sigmoid function θ_i and λ are picked such that at least one value of $(f2_{ij})$ is one for each (i) and $(ns_{ij}; j=1,2,... N_r)$.

C - Vertical Location Compatibility Factor $(f3_{ij})$

This measure is introduced to check if the matching points are on the same height in image planes. If the cameras are positioned on the same plane and they are identical then the matching points must be at the same height in their respective image planes. Therefore,

$$\begin{aligned}
f3_{ij} &= 1 && \text{if feature points } i \text{ and } j \text{ are at the same height} \\
f3_{ij} &= -1 && \text{if feature points are not at the same height}
\end{aligned} \tag{3.10}$$

4. DETERMINATION OF 3-D COORDINATES

The point where the lines of sight of the matching feature points intersect is the location of the object point in space. However, if the cameras are not ideal pin-hole cameras, as in the case of real world cameras, then it is impossible to construct the line of sight because there is no well defined focal point. This problem is solved by using the 2-plane calibration technique [4]. This methodology can be described within the following steps:

- (i). A plane with a set of object points is mounted vertically within the working space of the camera. The location of the object points are measured with respect to a fixed coordinate frame and recorded as $O_i \in R^3$. Corresponding locations on the camera image plane coordinate frame are measured and recorded as $I_i \in R^2$.
- (ii). Using the least squares algorithm, a polynomial fit is obtained between O_i and I_i as

$$O_{ij} = h_1(I_{ij}) \tag{3.11}$$

(iii). Following the previous steps, a second plane is mounted vertically in a different location within the working space and a similar least squares fit is obtained as

$$O_{2i} = h_2(I_{2i}) \quad (3.12)$$

(iv). For any given feature point I_i , the equations (3.11) and (3.12) are used to determine two points in space as $O1_i$ and $O2_i$. The line passing through $O1_i$ and $O2_i$ is used as the line of sight. This procedure is further illustrated in **Figure 5**.

(v). For every feature point on the left and right image planes, a line of sight is determined. If the lines of sight intersect then the intersection point is assumed as the object point in space. If the line of sights do not intersect, the mid-point between the lines where they pass closest to each other is taken as the corresponding object point location.

5. EXAMPLE

The left and right images of a test object are given in **Figures 6 and 7**. The imaging system has a resolution of 8 bits/gray tone. The effect of the LOG filter on the original images are shown in **Figures 8 and 9**. The black dots are the location of zero crossing points that are obtained by an LOG filter operating with $\sigma=7$. A user defined threshold band is used to eliminate the noise induced zero-crossings. If the average of the LOG values immediately before and after the zero crossing does not exceed a user specified threshold value then this zero crossing is assumed to be caused by noise and is not considered. The threshold level used is 7. All zero crossings are categorized following the procedure outlined in Step 2 of Section 2. Each horizontal line is examined first. If a zero crossing is detected with a sign change from positive to negative, its category is noted as 1. If a sign change is from negative to positive then its category is 2. Similarly, all columns are checked from top to bottom. If a zero crossing point is not categorized in the horizontal scanning, then a sign change from positive to negative makes this point of category 3, otherwise 4. The feature points are then determined by selecting the zero crossing points of category 1 on five selected lines. They are also shown with their label numbers in **Figures 8 and 9**.

Tables 1 and 2 give the image plane coordinates of the labeled feature points. **Table 3** lists the minimum distances between the lines of sight of feature points. The information in the table is a global information in matching because if the distance is zero then (i) and (j) are exact matching points. **Table 4** shows the non-similarity measures which indicate how similar the environment around the feature points.

Table 5 lists the θ and λ parameters of the compatibility factors ($f1_{ij}$) and ($f2_{ij}$). Note that these parameters are optimized for each feature point as shown in (3.5) and (3.9). Finally, **Table 6** contains the compatibility factors (C_{ij}) obtained by (3.2). The weights used in evaluating the compatibility factors are $W1=0.5$, $W1=0.35$ and $W1=0.15$.

The task of the Hopfield neural network is to determine the matching image points based on the compatibility values (C_{ij}). The neural network is shown in **Figure 10**. The steady state solution of the network with (1) initial conditions are given in **Table 7**. The numeric entry (1) indicates that the feature points (i) and (j) are the matching points. The (0) entry signifies no match between the feature points.

Once the matching feature points are determined, the locations of the object points are calculated by the lines of sight. The calculated three dimensional coordinates of the object points and the measured coordinates agree with each other as shown in **Table 8**. The entries marked by (?) in the table indicate that only two feature points are falsely matched by the network.

Error Analysis:

Analyzing the error in the same order as the process, the first potential source of error is due to image acquisition. The imaging board used can only sample a finite number of image points (256X256) with a finite resolution (6 bits/gray level). As a result of this limitation, a 2 plane camera calibration equations (3.11) and (3.12) are effected by two different errors; one is due to the discretized location of the image point and two is due to the finite number of terms used in the polynomial fit. A maximum error of 4 mm. occurred in the camera calibration in our experiments. In other words, the exact location of the object point is miscalculated by at most 4 mm. through calibration equations.

The LOG filter blurs the image therefore, causes the calculated edge points (zero crossings) to shift with respect to the actual edge points observed on the image. The direction and the amount of this shift are nonlinear functions of the environment and the bandwidth of the filter σ . It is difficult to quantify this shift but it can be minimized by choosing σ as small as possible. Furthermore, the amount of shift is expected to be the same for matching points since both images are convolved with the same size LOG filter.

The outcome of the Hopfield type optimizing neural network depends on the weight parameter (A) of the energy equation (3.1). Too small a value for (A) puts unnecessarily more emphasis on the constraint terms therefore may create mismatches. On the other hand, too large a value for (A) may create more than one match for a given feature point. For the example presented, A=15 gives good matching results.

6. CONCLUSIONS

This paper proposes a Hopfield type neural network in order to solve the matching problem in stereo imaging. The network offers a parallel computing architecture and minimizes a performance index that penalizes the mismatch. The methodology starts with the left and right hand images of a given object. The images are first filtered by a Laplacian of Gaussian (LOG) filter in order to detect a set of feature points. The feature points on the left and the right images are then matched using a Hopfield type optimization network. The performance index of the Hopfield network contains both local and global properties of the feature points and discourages multiple matches for a given feature point. The technique is demonstrated on a real object and sources of errors are discussed.

REFERENCES

1. Nasrabadi, M. N. and Li, Wei, "Object Recognition by a Hopfield Neural Network", IEEE Transactions on Systems, Man, and Cybernetics, Vol. 21, No. 6, pp. 1523-1535, December 1991.

2. Nasrabadi, M. N., Choo, C. Y., "Hopfield Network for Stereo Vision Correspondence", IEEE Transactions on Neural Networks, Vol. 3 No.1, January 1992.
3. Kasparian V.S., Batur, C., Duval, W.M.B, Rosenthal, B.N., Singh, N B "Application of Stereo Imaging for Recognition of Crystal Surface Shapes", in press, Journal of Crystal Growth.
4. Gonzalez R. C. ., Woods R. E. Digital Image Processing, pp 67-68. Addison Wesley 1993.
5. Baker, H. H. and Binford, T. D., "Depth from Edge and Intensity Based Stereo", Proc. Seventh Int. Joint Conf. Artificial Intell., pp. 631-636, August 1981.
6. Mayhew, J. E. W. and Frisby J. P., "Psychophysical and Computational Studies towards a Theory of Human Stereopsis", Artificial Intelligence, 17, pp. 349-385, 1981
7. Bernard, T. S. and Thompson, W. B., " Disparity Analysis of Images", IEEE Trans. Pattern Anal. Machine Intell., Vol. PAMI-2, No.4, pp. 333-340, July 1980.
8. Nasrabadi, N. and Liu, Y., " Application of Multichannel Hough Transform to Stereo Vision", Proc. SPIE Advances in Intelligent Robotics System, Vol. 848, November 1987.
9. Medioni, G. and Nevatia, R., " Segment Based Stereo Matching", Comp. Vision and Image Processing Vol. 31, pp. 2-18, 1985.
10. Moravec, H., "Robot Rover Visual Navigation", Ann Arbor, MI: U.M.I. Research Press, 1981.
11. Marr, D., Vision. W.H. Freeman and Company, San Fransisco, 1982.

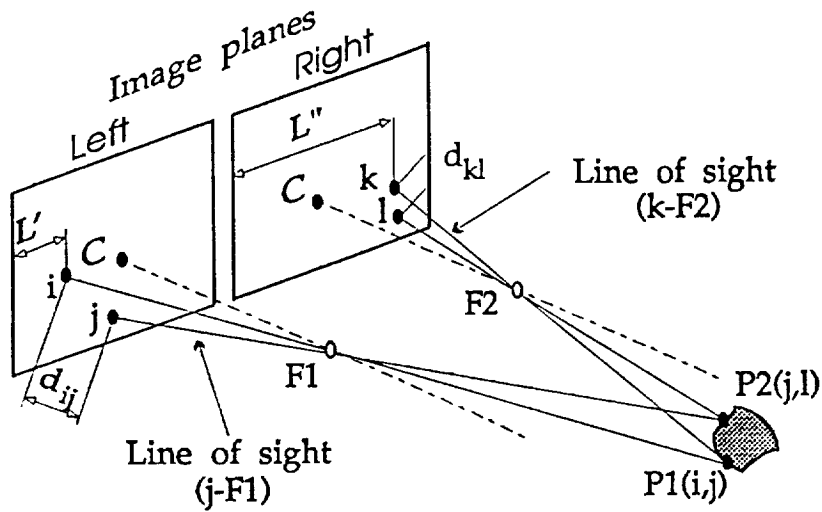


Figure 1. Stereo imaging Procedure

The point (i) on the left image matches point (k) on the right image, and simultaneously, the point (j) on the left image matches point (l) on the right image

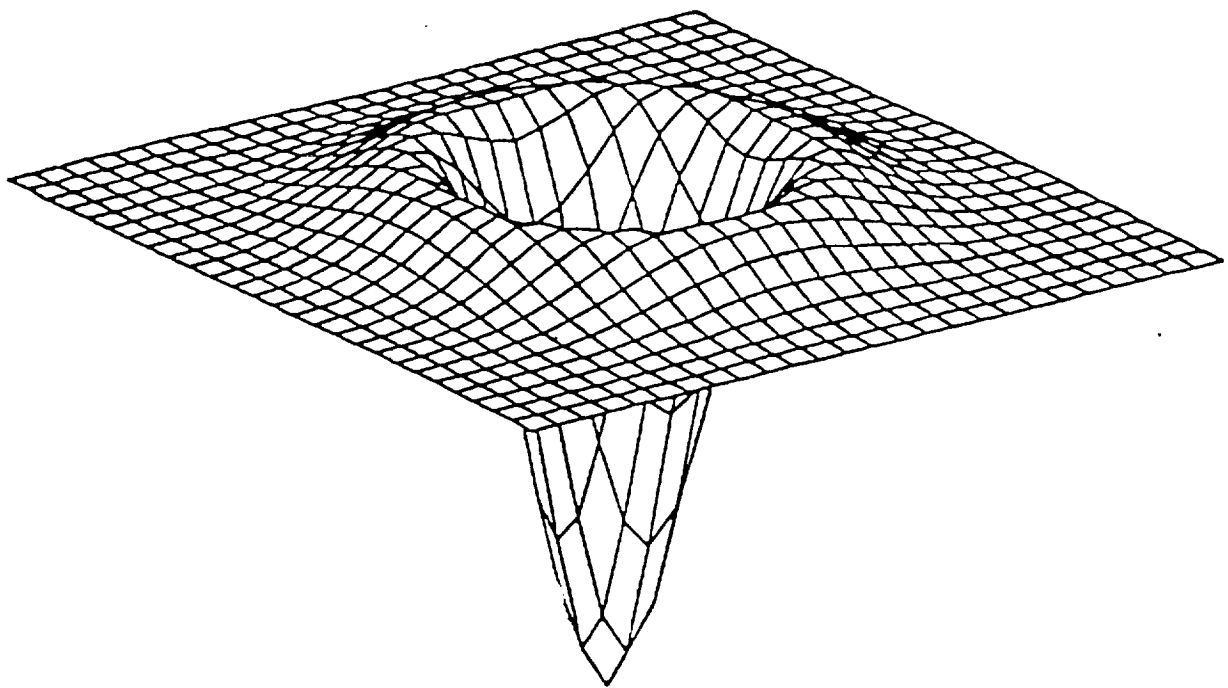


Figure 2. The shape of the LOG filter.

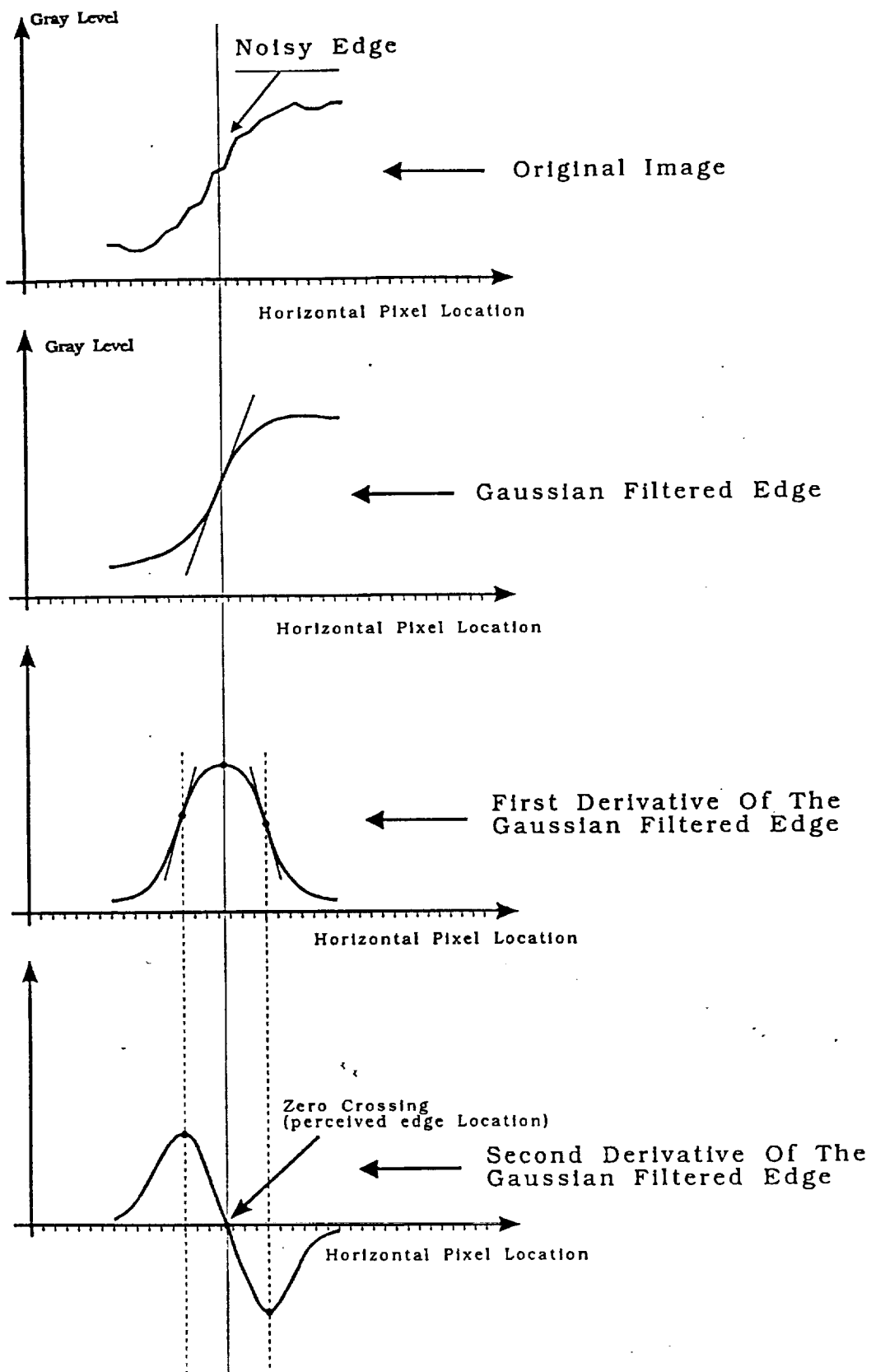


Figure 3. Detection of an edge, one dimensional case.

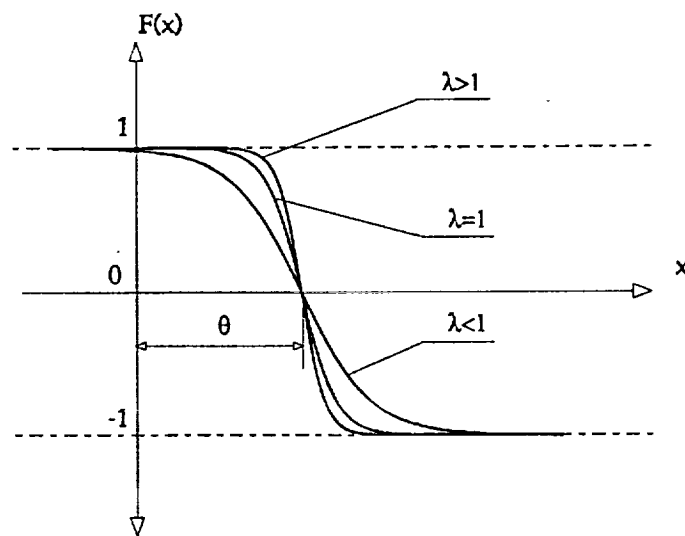


Figure 4: Sigmoid function for determination of compatibility factors

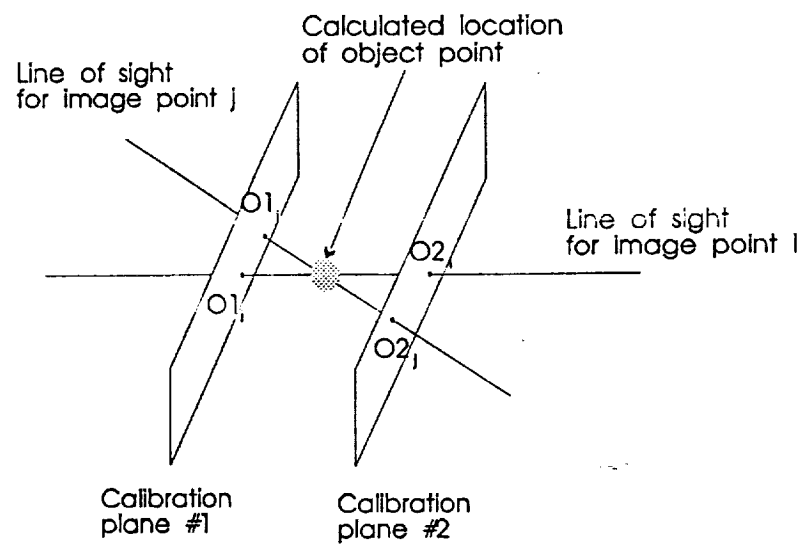


Figure 5: 2-Plane camera calibration



Figure 7. The right image



Figure 6. The left image

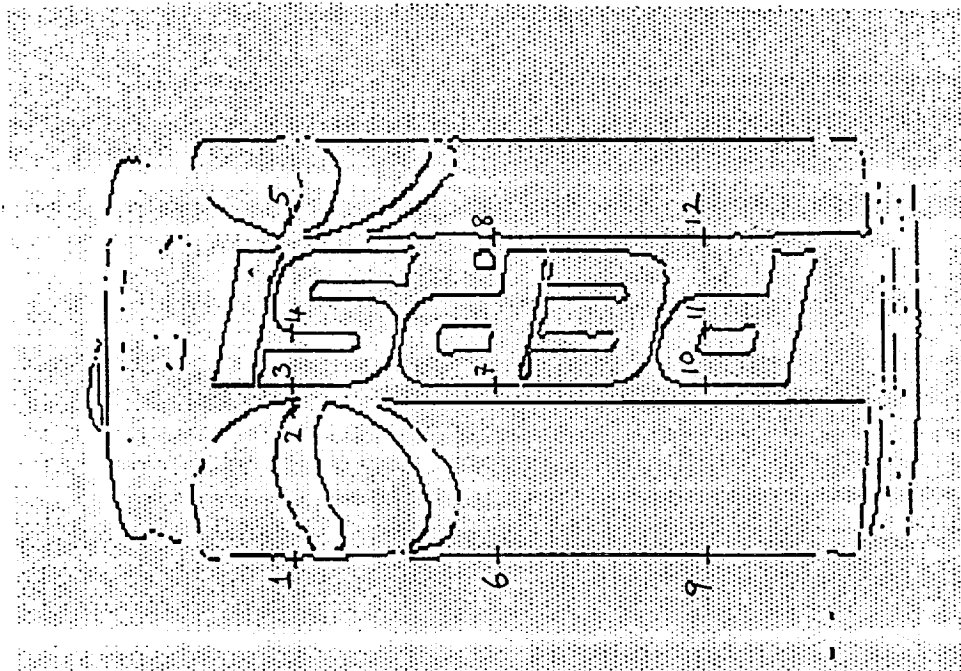


Figure 8. The left image.

The LOG filter is implemented and feature points are extracted

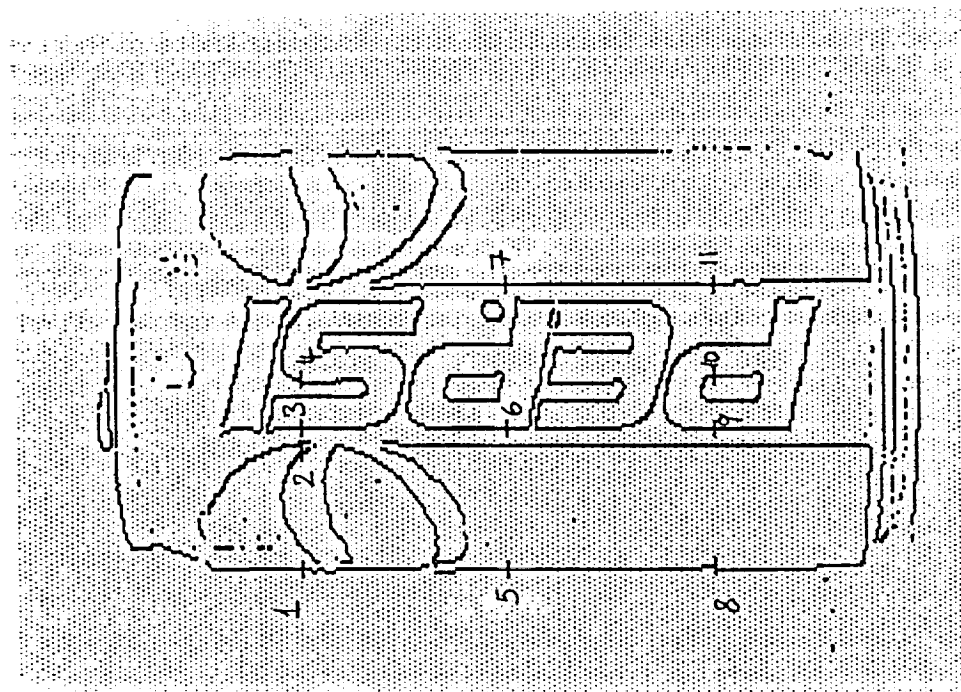


Figure 9. The right image.

The LOG filter is implemented and feature points are extracted

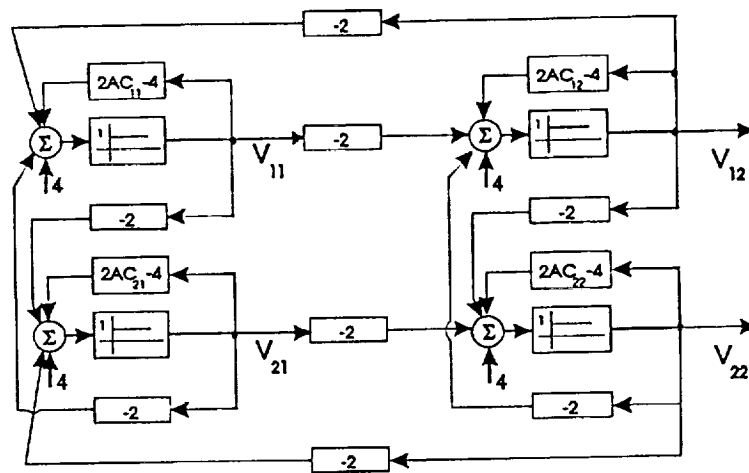


Figure 10: Schematic of the neural network, shown for four neurons

LABEL	X1	Y1	Z1
1	277	99	1
2	320	99	1
3	327	99	1
4	342	99	1
5	278	173	1
6	327	173	1
7	370	173	1
8	278	247	1
9	327	247	1
10	343	247	1
11	370	247	1

Table 1. Left image feature points and image plane coordinates.

LABEL	X2	Y2	Z2
1	84	110	1
2	117	110	1
3	124	110	1
4	138	110	1
5	84	189	1
6	124	189	1
7	165	189	1
8	85	268	1
9	124	268	1
10	139	268	1
11	165	268	1

Table 2. Right image feature points and image plane coordinates.

i/j	1	2	3	4	5	6	7	8	9	10	11
1	0.01	14.15	14.18	14.26	3.10	3.90	5.16	5.51	6.42	6.83	7.59
2	14.09	0.00	0.01	14.06	2.54	3.08	3.86	4.78	5.49	5.81	6.43
3	14.10	0.02	0.00	0.04	2.47	2.98	3.71	4.69	5.36	5.67	6.26
4	14.12	0.04	0.03	0.00	2.34	16.79	3.42	4.49	5.11	5.39	5.93
5	3.17	3.68	3.82	4.13	0.01	14.06	14.10	3.14	3.85	4.21	5.02
6	2.64	2.95	3.03	3.21	14.01	0.02	14.04	2.59	3.03	3.25	3.69
7	2.31	2.53	2.58	2.70	14.00	14.02	0.04	2.28	2.60	2.75	3.04
8	5.65	6.36	6.50	6.90	3.12	3.85	5.08	0.01	14.05	14.10	14.24
9	4.80	5.32	5.44	5.71	2.52	2.97	3.66	14.08	0.05	0.02	14.04
10	4.58	5.04	5.15	5.39	2.37	2.76	3.35	14.10	0.08	0.06	14.00
11	4.24	4.63	4.72	4.92	2.15	2.46	2.91	14.14	14.12	14.11	0.07

Table 3. Minimum distance between the lines of sight.

i/j	1	2	3	4	5	6	7	8	9	10	11
1	431	512	439	567	403	647	485	506	554	374	357
2	559	210	601	655	568	765	640	529	739	481	533
3	276	614	158	541	276	367	208	569	417	410	232
4	566	693	451	334	508	427	381	686	369	531	580
5	181	518	249	537	101	372	210	449	400	337	217
6	399	751	367	442	406	14	186	744	157	583	394
7	421	613	372	572	408	572	409	592	519	448	440
8	96	473	164	494	96	287	125	444	357	294	132
9	501	701	377	367	448	182	281	689	116	515	499
10	476	484	458	621	423	647	495	486	585	283	435
11	151	505	239	525	171	287	200	489	362	350	121

Table 4. Non-similarity measures.

		i=1	i=2	i=3	i=4	i=5	i=6	i=7	i=8	i=9	i=10	i=11
For f1 _{ij}	Θ_i	1.005	1.000	1.000	1.000	1.005	1.010	1.020	1.005	1.010	1.030	1.035
	λ_i	5.319	5.293	5.293	5.293	5.319	5.346	5.401	5.319	5.346	5.457	5.485
For f2 _{ij}	Θ_i	360	213	161	337	104	17	375	99	119	291	124
	λ_i	3	3	3	3	3	3	3	3	3	3	3

Table 5. Optimized parameters for the compatibility factors.

i/j	1	2	3	4	5	6	7	8	9	10	11
1	0.29	-0.70	-0.70	-0.70	-1	-1	-1	-1	-1	-1	-0.30
2	-0.70	0.99	0.28	-0.70	-1	-1	-1	-1	-1	-1	-1
3	-0.70	0.28	0.99	0.28	-1	-1	-1	-1	-1	-1	-1
4	-0.70	0.28	0.28	0.99	-1	-1	-1	-1	-1	-1	-1
5	-1	-1	-1	-1	0.99	-0.70	-0.70	-1	-1	-1	-1
6	-1	-1	-1	-1	-0.70	0.99	-0.70	-1	-1	-1	-1
7	-1	-1	-0.30	-1	-0.70	-0.70	0.29	-1	-1	-1	-1
8	-0.30	-1	-1	-1	-0.30	-1	-1	0.29	-0.70	-0.70	-0.70
9	-1	-1	-1	-1	-1	-1	-1	-0.70	0.99	0.29	-0.70
10	-1	-1	-1	-1	-1	-1	-1	-0.70	0.29	0.99	-0.70
11	-1	-1	-1	-1	-1	-1	-1	-0.70	-0.70	-0.70	0.99

Table 6. Overall compatibility values (C_{ij}).

i/j	1	2	3	4	5	6	7	8	9	10	11
1	1	0	0	0	0	0	0	0	0	0	0
2	0	1	0	0	0	0	0	0	0	0	0
3	0	0	1	0	0	0	0	0	0	0	0
4	0	0	0	1	0	0	0	0	0	0	0
5	0	0	0	0	1	0	0	0	0	0	0
6	0	0	0	0	0	1	0	0	0	0	0
7	0	0	0	0	0	0	1	0	0	0	0
8	0	0	0	0	0	0	0	1	0	0	0
9	0	0	0	0	0	0	0	0	1	1	0
10	0	0	0	0	0	0	0	0	1	1	0
11	0	0	0	0	0	0	0	0	0	0	1

Table 7. The steady state solution of the neural network.

PAIR	CALCULATED COORDINATES			REAL COORDINATES + 0.5		
	X	Y	Z	X	Y	Z
1,1	8.73	9.35	49.54	8.7	9.25	49
2,2	6.58	9.13	46.61	6.6	9.25	46
3,3	6.37	8.98	44.74	6.25	9.25	46
4,4	5.47	9.12	46.34	5.50	9.25	46
5,5	8.69	6.03	49.07	8.70	6.00	49
6,6	6.23	5.98	46.43	6.20	6.00	46
7,7	4.07	5.99	45.91	4.00	6.00	45.7
8,8	8.68	2.74	49.22	8.70	2.75	49
9,9	6.24	2.85	46.26	6.20	2.75	46
9,10	5.87	2.72	50.84	?	?	?
10,9	5.81	2.97	42.16	?	?	?
10,10	5.44	2.86	46.00	5.40	2.75	46
11,11	4.08	2.88	45.75	4.00	2.75	45.7

Table 8. Calculated and measured 3-D coordinates of the object points